Modelling and Optimization of the Electrical Parameters of an $In_xGa_{1-x}N$ Solar Cell Under Dynamic Frequency Illumination

Baboucar Fickou, Moussa Camara, Moustapha Thiame(✉), Issa Faye, Landing Diatta, and Mamadou Faye

Assane Seck University of Ziguinchor, LCPM, Ziguinchor, Senegal
{m.camara1696,m.faye20160903}@zig.univ.sn, {mthiame, issa.faye}@univ-zig.sn

Abstract. In this article, we propose a modelling and optimization of an $In_xGa_{1-x}N$ based PV solar cell in the frequency-dynamic regime under monochromatic illumination.

We first elaborated a mathematical model of the $In_xGa_{1-x}N$ based solar cell in order to study its behaviour when subjected to monochromatic illumination in the frequency-dynamic regime. We were able to establish the electrical parameters as a function of the pulsation and wavelength of the illumination.

Next, we optimized the indium proportion as a function of the nature of the illumination by simulating the efficiency of the PV solar cell, for different wavelength of the illumination and values of the pulsation, as a function of the indium fraction. This enabled us to obtain, for an illumination pulsation ranging from 0 to 10^6 rad. s^{-1}, the optimum values for the indium fraction, which are $x_{op} = 0.28$ and $x_{op} = 0.26$ respectively for wavelengths of 0.5 μm and 0.9 μm, corresponding to optimum efficiencies of 28.7% and 26.6% respectively. Above a pulsation of 10^6 rad. s^{-1}, the increase in pulsation leads to an increase in the indium fraction, resulting in a decrease in efficiency for both short and long wavelengths.

Keywords: Frequency · Optimization · Efficiency · Wavelength · Optimum indium fraction

1 Introduction

Fossil fuels, which emit high levels of carbon dioxide (CO_2), account for the vast majority of the world's energy consumption. These fuels account for almost 85% of the world's energy consumption. Renewable energies (wind, photovoltaic) account for around 3% of global consumption [1]. To reduce the use of these polluting energies, the share of renewable energies in the energy mix should be considerably increased. Huge efforts are currently being made worldwide to develop these 'clean' renewable energies.

There are many expectations in the photovoltaic (PV) sector: increased conversion efficiency, lower production costs, reduced environmental impact, and so on. Currently,

K. Cheikh M. F. Kebe et al. (Eds.): InterSol 2024, LNICST 610, pp. 38–46, 2025.
https://doi.org/10.1007/978-3-031-86493-3_4

the PV filière is largely dominated by crystalline silicon technology, with almost 93% of global production in 2016 [2]. However, the production of silicon-based PV solar cells remains costly and requires a large quantity of materials. In addition, silicon solar cells currently have a maximum laboratory efficiency of 25.6% [3], which is very close to the maximum theoretical limit for a single-junction cell [4]. As a result, the growing need for photovoltaic energy has prompted research into the use of other alternative materials, although this in no way means that research in the silicon field has come to a halt. Today, this wide-ranging research is focused mainly on thin-film technologies. These include technologies based on III-V materials, which are highly promising in terms of efficiency. InGaN alloys have a direct and variable band gap from 3.42 eV to 0.76 eV that covers the entire solar spectrum. They have a very high coefficient of absorption (10^5 cm-1) so that a few hundred nanometers of thickness are suffiscient for absorbing the majority of incident light. This alloy began to emerge as a promising material for PV applications after its considerable developments for light-emitting diode (LED) blues [5]. With the aim of contributing to the optimization of the electrical parameters of InGaN-based solar cells, we propose in this work the modelling and optimization of an $In_xGa_{1-x}N$-based solar cell under monochromatic illumination in a dynamic frequency regime. A mathematical model will be proposed to obtain the various parameters of the solar cell.

Finally, using simulation, we will propose an optimization method to
Obtain the best performance from the solar cell.

2 Mathematical Modelling

2.1 Introducing the Solar Cell

In this study, we consider a solar cell as shown in Fig. (1). The parameter H designates the thickness of the cell base. In practice, the dimensions of the base along the axes perpendicular to the z axis are very large compared with the depth of the solar cell. Thus, the current is neglected by these directions. By hypothesis, the diffusion coefficient of the minority carriers in the emitter is considered negligible compared with that of the base. Thus, our analysis is developed only on the base of the solar cell. We also take the origin of our reference frame from the emitter of the solar cell [6].

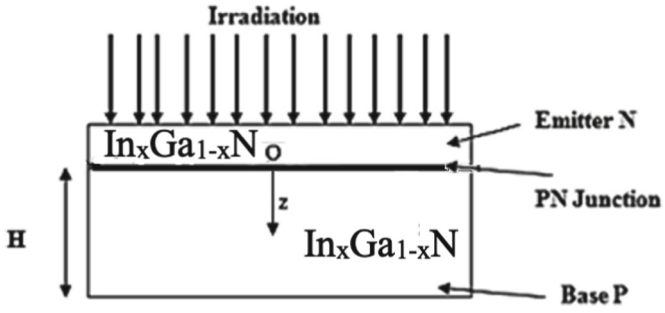

Fig. 1. Presentation of the $In_xGa_{1-x}N$ based solar cell subjected to frequency illumination

2.2 Optical Parameters

Our study is based on ($In_xGa_{1-x}N$), where the magnitude x represents the indium fraction. The solar energy band gap is related to the indium fraction as follows [7].

$$Eg = x \cdot Eg^{InN} + (1 - x) \cdot Eg^{GaN} - b \cdot x \cdot (1 - x) \tag{1}$$

where the energy of the band gap of l'InN (Eg^{InN}) et GaN (Eg^{GaN}) are respectively 0,7 eV et 3,42 eV et b = 1,43 eV.

The absorption coefficient is also given as a function of the indium fraction and the incident photon as follows [8]:

$$\alpha(\lambda, x) = 10^5 \sqrt{C(x)\left(E_{ph} - E_g(x)\right) + D(x)(E_{ph} - E_g(x))^2} \tag{2}$$

where Eph = 1,24/λ represents the energy of the photon and λ the wavelength.

$$c = 3{,}525 - 18{,}29 \cdot x + 40{,}22 \cdot x^2 - 37{,}52 \cdot x^3 + 12{,}77 \cdot x^4 \tag{3}$$

$$D = -0{,}6651 + 3{,}616 \cdot x - 2{,}46 \cdot x^2 \tag{4}$$

The refractive index of the solar cell is given as a function of the photon energy and the indium fraction as follows [9, 10]:

$$N(\lambda, x) = \sqrt{A(x) \cdot \left(\frac{E_g}{E_{ph}}\right)^2 \cdot \left[2 - \sqrt{1 + \frac{E_{ph}}{E_g}} - \sqrt{1 - \frac{E_{ph}}{E_g}}\right] + B(x)} \tag{5}$$

where

$$A(x) = 13{,}55 \cdot x + 9{,}31 \cdot (1 - x);\ B = 2{,}05 \cdot x + 3{,}03 \cdot (1 - x) \tag{6}$$

2.3 Electronic Parameters

The concentration of intrinsic carriers is also given by the indium fraction and takes the following form [10]:

$$n_i = \sqrt{N_c \cdot N_v} \cdot e^{\frac{-E_g}{2 \cdot K_b \cdot T}} \tag{7}$$

With Nc and Nv being the density of state in the conduction band and valence band respectively. Their expressions are given respectively in the form:

$$N_c = (0{,}9 \cdot x + 2{,}3 \cdot (1 - x)) \cdot 10^9 (IV - 8) \tag{8}$$

$$N_v = (5{,}3 \cdot x + 1{,}8 \cdot (1 - x)) \cdot 10^{19} \tag{9}$$

The follows equation give the expression of the carrier's effective mass [8]

$$m_n = (0{,}12 \cdot x + 0{,}2 \cdot (1 - x)) \cdot m_0 \tag{10}$$

The intrinsic diffusion coefficient used in the simulation is [10]:

$$D_0 = \frac{K_b \cdot \tau \cdot T}{(0{,}12 \cdot x + 0{,}2 \cdot (1 - x) \cdot m_0} \tag{11}$$

2.4 Continuity Equation

The equation governing the variation in the density of photo-generated minority charge carriers in the base of a photovoltaic cell in static equilibrium is [11]:

$$D(\omega) \times \frac{\partial^2 \delta(z, t)}{\partial z^2} - \frac{\delta(z, t)}{\tau} = -G(z, \alpha, w, t) + \frac{\partial \delta(z, t)}{\partial t} \tag{12}$$

With:

δ (z, t) is the minority carrier density as a function of space z and time.

$$\delta(z, t) = \delta(z).e^{-j.\omega.t} \tag{13}$$

G (z, α, ω, t) is the generation rate of carriers.

$$G(z, \alpha, \omega, t) = g(z, \omega).e^{-j.\omega.t} \tag{14}$$

with.

$$g(z, \omega) = \alpha(\lambda, x).I_0(\lambda).(1 - R(\lambda, x)).e^{-\alpha(\lambda, x).Z} \tag{15}$$

where:

$I_0(\lambda)$ is the intensity of the incident monochromatic light.

R (λ, x) and α (λ, x) are the reflection and absorption coefficients respectively.

The continuity equation becomes, by replacing the Eq. (14) and (15) in (16):

$$\frac{\partial^2 \delta(z, t)}{\partial z^2} - \frac{\delta(z, t)}{L^2(\omega)} = -\frac{g(z, \omega)}{D(\omega)} \tag{16}$$

L(ω) is the complex of the diffusion length in the base [7],

$$L(\omega) = \sqrt{\frac{D(\omega).\tau}{1 + j.\omega.\tau}} \tag{17}$$

The solution to this equation gives:

$$\delta(z, \omega) = A \cdot \cosh\left(\frac{z}{L(\omega)}\right) + B \cdot \sinh\left(\frac{z}{L(\omega)}\right) + K \cdot e^{-\alpha(\lambda, x) \cdot z} \tag{18}$$

with:

$$K = \frac{\alpha(\lambda, x) \cdot I_0(\lambda, x) \cdot (1 - N(\lambda, x)) \cdot [L(\omega)]^2}{D(\omega)\left[L(\omega)^2 \cdot \alpha^2 - 1\right]} \tag{19}$$

The coefficients A and B are determined through the boundary conditions [10]:

- At the junction:

$$D(\omega) \cdot \left.\frac{\partial \delta(z, \omega)}{\partial Z}\right|_{z=0} = S_f \cdot \delta(z, \omega)\big|_{z=0} \tag{20}$$

- on Back face:

where Sf and Sb are the recombination speeds at the junction and at the back of the solar cell, respectively.

$$\mathrm{D}(\omega) \cdot \left.\frac{\partial \delta(z,\omega)}{\partial z}\right|_{z=H} = -S_b \cdot \delta(z,\omega)|_{z=H} \tag{21}$$

As a function of the minority carrier density in the base, the photocurrent density is given by the expression (22) [11]:

$$\mathrm{J_{ph}} = \mathrm{q} \cdot \mathrm{D}(\omega) \cdot \left.\frac{\partial \delta(z,\omega)}{\partial z}\right|_{z=0} \tag{22}$$

When the solar cell is illuminated, a photovoltage is produced, the expression for which is given by Boltzmann's Eq. (23) [12]:

$$\mathrm{V_{ph}} = V_T \cdot \ln \cdot \left(1 + \frac{N_b}{n_0^2} \cdot \partial \delta(z,\omega)\Big|_{z=0}\right) \tag{23}$$

The diode current is a leakage current which characterizes the losses of charge carriers.

photogenerated. It is given by the following relationship [13]:

$$Id\left(S_f,\omega\right) = q \cdot S_f \cdot \frac{n_0^2}{N_b}\left(e^{\left(\frac{V_{ph}\left(S_f,w\right)}{V_T}\right.} - 1\right) \tag{24}$$

Equations (22), (23) and (24) give the expression for the electrical power supplied by the solar cell for monochromatic illumination:

$$P(Sf,\omega) = \left(\mathrm{Jph}\left((Sf,\omega) - Id\left(S_f,\omega\right)\right)\right) \times V_{ph}(Sf,\omega) \tag{25}$$

3 Results and Discussion

3.1 Power Study

Figure (2) shows the power as a function of the recombination rate for different frequency values.

These power profiles as a function of the recombination rate Sf can be analysed along three axes:

- For values of Sf between 0 and 2.10^2 cm.s^{-1} the power is almost zero, which can be explained by the fact that at this speed range the photocurrent density is low or even zero due to the proximity of the open circuit [6].

- From 3.10^2 to 4.10^4 cm.s^{-1} the power increases progressively until it reaches its maximum value, which corresponds to the maximum power of the solar cell.

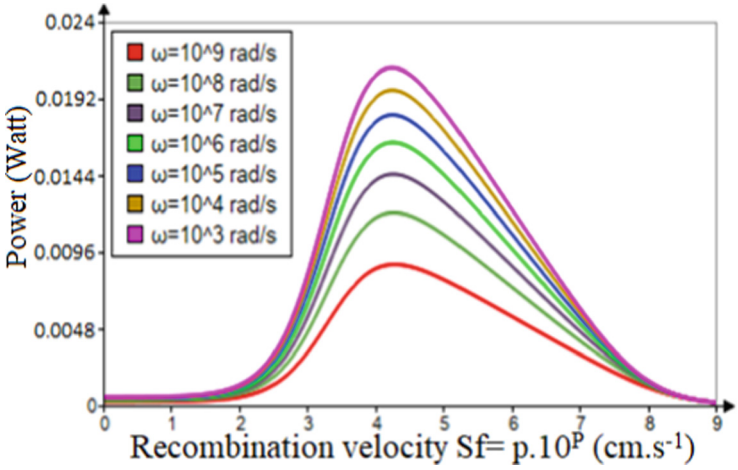

Fig. 2. Power as a function of recombination speed for different modulation frequency values (H = 3 μm, λ = 0,5 μm, x = 0,3, Sb = 2.10^2 $cm.s^{-1}$).

- Above 4.10^4 $cm.s^{-1}$ the power decreases sharply until it is completely cancelled out. This can be explained by the fact that as the solar cell approaches the short-circuit operating point, the voltage will tend towards zero [12].

We can also see that the maximum power value decreases with frequency. So we can say that an increase in frequency leads to a decrease in power.

3.2 Optimization of the Indium Fraction as a Function of the Pulsation and Wavelength of the Illumination

Our approach consists of simulating the efficiency of our solar cell for a wavelength λ equal to 0.5 μm and 0.9 μm as a function of the indium fraction for different frequency values. This method will enable us to obtain the optimum values for the indium fraction and the frequency, which will give the highest efficiency.

Figures (3) and (4) show the variation of the photocell efficiency as a function of the indium fraction for different values of the frequency for wavelengths λ = 0.5 μm and λ = 0.9 μm respectively.

In Figs. (3, 4), as the indium fraction increases, we note an increase in the efficiency until it reaches a maximum which corresponds to its optimum value for a fixed frequency and wavelength. We also note that the maximum efficiency decreases as the frequency increases beyond 10^6 $rad.s^{-1}$. This is because high frequencies do not allow minority carriers to diffuse, as many of them will be recombined either in the bulk or on the surface of the solar cell. This explains the decrease in the diffusion coefficient [12], which means that the maximum efficiency decreases with frequency.

For a given frequency, the optimum indium fraction is obtained when the conversion efficiency reaches its maximum. Tables 1 and 2 summarise the optimum values for the indium fraction at wavelengths of 0.5 μm and 0.9 μm respectively, as well as the optimum electrical parameters of the solar cell as a function of pulsation: short-circuit

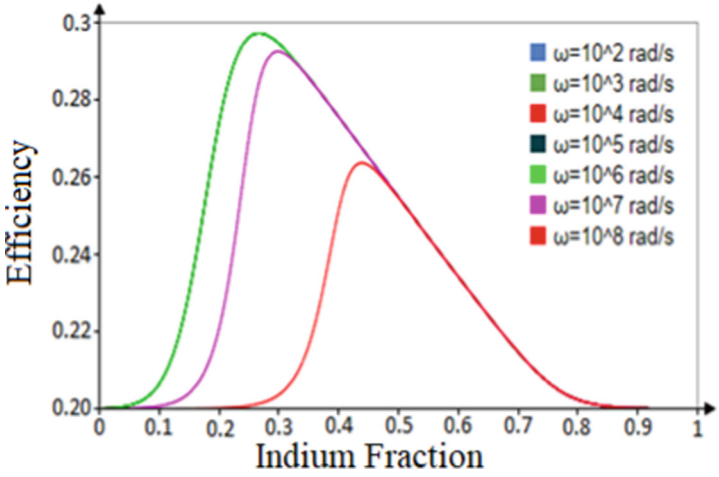

Fig. 3. Cell efficiency as a function of indium fraction for different frequency values ($\lambda = 0.5$ μm, H = 3 μm, Sf = 6.10^6 cm.s^{-1}, Sb = 2.10^2 cm.s^{-1}.)

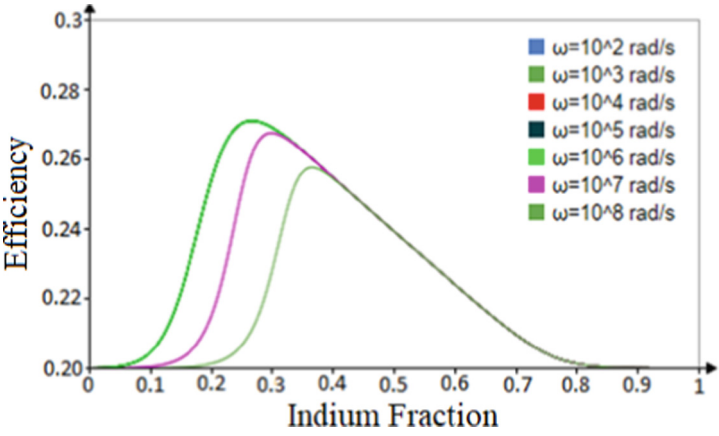

Fig. 4. Efficiency as a function of indium fraction for different frequency values ($\lambda = 0.9$ μm, H = 3 μm, Sf = 6.10^6 cm.s^{-1}, Sb = 2.10^2 cm.s^{-1}).

current, open-circuit voltage, series and shunt resistances and conversion efficiency, for different frequencies of illumination.

We note that for both wavelengths, we have an increase in the optimum indium fraction for frequencies above 10^6 rad. s^{-1}. This corresponds to a decrease in the efficiency of the solar cell. On the other hand, for pulses ranging from 10^2 to 10^6, the optimum indium fraction is independent of frequency but decreases slightly as the length increases from 0.5 μm to 0.9 μm.

We also note that the optimum indium fraction is more sensitive to higher frequencies when the wavelength is short.

Table 1. Optimum values for the indium fraction and electrical parameters for $\lambda = 0{,}5\ \mu m$

ω(rad/s)	X_{op}	$Jcc_{op}(A/cm^2)$	$Vco_{op}(V)$	$Rsh_{op}\ (\Omega.cm^3)$	$Rs_{op}\ (\Omega.cm^2)$	Ƞ (%)
10^2 to 10^6	0.28	0.071	3.8	$8.5\ 10^4$	0.3	28.7
10^7	0.30	0.048	3.6	$5.5\ 10^4$	0.26	28.6
10^8	0.44	0.033	2.7	$2.6\ 10^4$	0.18	26.3

Table 2. Optimum values for the indium fraction and electrical parameters for $\lambda = 0{,}9\ \mu m$

Ω (rad/s)	X_{op}	Jccop (A/cm^2)	$Vco_{op}(V)$	$Rsh_{op}\ (\Omega.cm^3)$	$Rs_{op}\ (\Omega.cm^2)$	Ƞ (%)
10^2 to 10^6	0.26	0.061	3.1	$4{,}5\ 10^4$	0.28	26.6
10^7	0.31	0.035	2.8	$2.7\ 10^4$	0.20	26.4
10^8	0.36	0.022	1.7	$1.6\ 10^4$	0.10	26.3

4 Conclusion

In this paper we have modelled the electrical parameters of a thin-film solar cell based on indium gallium nitride as a function of the pulsation and wavelength of the illumination. Simulation of the power as a function of the recombination rate at the junction for different pulsations shows that as the recombination rate increases, the productivity of the cell decreases.

We simulated the effect of the light modulation frequency and wavelength on the optimum indium fraction and on the power and efficiency of the solar cell.

For wavelengths equal to 0.5 μm and 0.9 μm, we obtained optimum values for the indium fraction x_{opt} equal to 0.28 and 0.26 respectively, corresponding to efficiencies equal to 28.6% and 26.6% respectively.

References

1. British Petroleum. BP statistical review of world energy. London: British Petroleum, 1 (2017)
2. Fraunhofer, I.S.E.: Photovoltaics report. Fraunhofer ISE, Freiburg **1**, 12–15 (2017)
3. Martin. A., Emery, G.K., Hishikawa, Y., Warta, W., Dunlop, E.D.: Solar cell efficiency tables (version 48). Progr. Photovolt.: Res. Appl. **24**(7), 905–913 (2016)
4. Shockley, W., Queisser, H.J.: Detailed balance limit of efficiency of p-n junction solar cells. J. Appl. Phys. **32**(3), 510–519 (1961)
5. Bhuiyan, A.G., Sugita, K., Hashimoto, A., et Yamamoto, A.: InGaN solar cells: present state of the art and important challenges, IEEE J. Photovolt.**2**(3), 276-293 (2012)
6. Ly, I., et al.: Techniques de détermination des paramètres de recombinaison et le domaine de leur validité d'une photopile bifaciale au silicium polycristallin sous éclairement multi spectral constant en régime statique. Revue des Energies Renouvelables (15), 187–206 (2012)
7. Benmoussa, D., Hassane, B., Abderrachid, H.: Simulation of $In_{0.52}Ga_{0.48}N$ Using AMPS ResearchGate, pp.1–5 (2017)

8. Mesrane, A., Rahmoune, F., Mahrane, A., et Oulebsir, A.: Design and Simulation of InGaN p - n Junction Solar Cell. Int. J. Photoenergy **2015**, 1–9 (2015)
9. Nawaz, M., Ahmad, A.: A TCAD-based modeling of GaN/InGaN/Si solar cells. Semicond. Sci. Technol. **27**(3), 019–035 (2012)
10. Pelap, F.B., Tagne, E.K., Kenfack, A.D.K.: Numerical optimization of a tandem solar cell based on InGaN. J. Renew. Energ. **24**, 25–39 (2021)
11. Ndiaye, M., et al.: Capacite de Diffusion d'une photopile au Silicium à Multijonction Verticales Connectées en Série sous Eclairement Monochromatique en Modulation de Fréquence : Effet du Taux de dopage de la Base. Int. J. Adv. Res. 10(4), 556–572 (2022)
12. Ly Diallo, H., et al.: Determination of the Recombination and Electrical Parameters of a Vertical Multijunction Silicon Solar Cell, pp.1–6 (2020)
13. Sow, O., Zerbo, I., Mbodji, S., Ngom, M.I., Diouf, M. S., Sissoko, G.: Silicon solar cell under electromagnetic waves in steady state: electrical parameters determination using the I-V and P-V characteristics. Int. J. Sci. Environ. Technol. **1**, 230–246 (2012)